

# Stoichiometry and arrangement of heteromeric olfactory cyclic nucleotide-gated ion channels

MARK S. SHAPIRO\* AND WILLIAM N. ZAGOTTA\*†‡

\*Department of Physiology and Biophysics and †Howard Hughes Medical Institute, Box 357290, University of Washington, Seattle, WA 98195-7290

Edited by Richard Winyu Tsien, Stanford University School of Medicine, Stanford, CA, and approved September 3, 1998 (received for review June 4, 1998)

**ABSTRACT** Native cyclic nucleotide-gated (CNG) channels are composed of  $\alpha$  and  $\beta$  subunits. Olfactory CNG channels were expressed from rat cDNA clones in *Xenopus* oocytes and studied in inside-out patches. Using tandem dimers composed of linked subunits, we investigated the stoichiometry and arrangement of the  $\alpha$  and  $\beta$  subunits. Dimers contained three subunit types:  $\alpha_{wt}$ ,  $\beta_{wt}$ , and  $\alpha_m$ . The  $\alpha_m$  subunit lacks an amino-terminal domain that greatly influences gating, decreasing the apparent affinity of the channel for ligand by 9-fold, making it a reporter for inclusion in the tetramer. Homomeric channels from injection of  $\alpha_{wt}\alpha_{wt}$  dimers and from  $\alpha_{wt}$  monomers were indistinguishable. Channels from injection of  $\alpha_{wt}\alpha_m$  dimers had apparent affinities 3-fold lower than  $\alpha_{wt}$  homomultimers, suggesting a channel with two  $\alpha_{wt}$  and two  $\alpha_m$  subunits. Channels from coinjection of  $\alpha_{wt}\alpha_{wt}$  and  $\beta\beta$  dimers were indistinguishable from those composed of  $\alpha$  and  $\beta$  monomers and shared all of the characteristics of the  $\alpha+\beta$  phenotype of heteromeric channels. Coinjection of  $\alpha_{wt}\alpha_m$  and  $\beta\beta$  dimers yielded channels also of the  $\alpha+\beta$  phenotype but with an apparent affinity 3-fold lower, indicating the presence of  $\alpha_m$  in the tetramer and that  $\alpha+\beta$  channels have adjacent  $\alpha$ -subunits. To distinguish between an  $\alpha-\alpha-\alpha-\beta$  and an  $\alpha-\alpha-\beta-\beta$  arrangement, we compared apparent affinities for channels from coinjection of  $\alpha_{wt}\alpha_{wt}$  and  $\beta\alpha_{wt}$  or  $\alpha_{wt}\alpha_{wt}$  and  $\beta\alpha_m$  dimers. These channels were indistinguishable. To further argue against an  $\alpha-\alpha-\alpha-\beta$  arrangement, we quantitatively compared dose-response data for channels from coinjection of  $\alpha_{wt}\alpha_m$  and  $\beta\beta$  dimers to those from  $\alpha$  and  $\beta$  monomers. Taken together, our results are most consistent with an  $\alpha-\alpha-\beta-\beta$  arrangement for the heteromeric olfactory CNG channel.

Cyclic nucleotide-gated (CNG) channels are best known for their role in sensory neurons in the transduction of external stimuli into an electrical signal (1–4). Since the initial cloning of CNG channels from retinal-rod photoreceptors (5) and from olfactory sensory neurons (6, 7), they have also been found to be expressed in testes, kidney, heart, and brain (8–11). It appears that many kinds of cells use CNG channels as part of their repertoire in shaping their response to extracellular signals and as a mode of  $Ca^{2+}$  entry (12). In olfactory receptor neurons, cell-surface receptors that recognize a vast array of odorants use a G protein-mediated signaling pathway to stimulate adenylyl cyclase, and the resulting increase in cAMP concentration opens CNG channels (4). Cation influx through CNG channels depolarizes the cell and increases intracellular  $Ca^{2+}$  concentrations (13). Both the olfactory and rod classes of CNG channels are also found in the hippocampus (11), where they may play a role in memory and learning (14).

The putative topology of all known CNG subunits is similar to voltage-gated  $K^+$  channels, with six membrane-spanning segments and a pore-forming P region. CNG channels, however, have an additional cyclic nucleotide-binding domain in their

intracellular carboxyl-terminal region that exhibits sequence similarity to other cyclic nucleotide-binding proteins. Recently, the amino-terminal region of the olfactory  $\alpha$ -subunit has been shown to potentiate channel activation by interaction with the carboxyl-terminal region (15).  $Ca^{2+}$ /calmodulin inhibits these channels by binding to the amino-terminal domain and preventing this auto-excitatory interaction (15, 16).

Like  $K^+$  channels, CNG channels are thought to form as tetramers of four subunits arranged around a central, ion-conducting pore (17–19). Native rod and olfactory CNG channels are thought to be composed of at least two types of subunits,  $\alpha$  and  $\beta$  (20–22). The olfactory  $\beta$ -subunit exhibits 52% sequence identity to the  $\alpha$ -subunit and 30% sequence identity to the rod  $\beta$ -subunit. It is expressed throughout the nasal epithelium, especially in olfactory sensory neurons, and in the vomeronasal organ (20, 22, 23). The olfactory  $\beta$ -subunit does not form cyclic nucleotide-activatable channels by itself. However, incorporation of the  $\beta$ -subunit into heteromeric channels with the  $\alpha$ -subunit has a profound effect on the behavior of the olfactory channel, greatly increasing the apparent affinity for cAMP, as well as altering its voltage-dependence and rectification properties (20, 22).

We wished to ascertain the stoichiometry and arrangement of the subunits of heteromeric  $\alpha+\beta$  olfactory CNG channels. Our approach was to generate tandem dimer constructs containing two subunits placed in tandem in a single open reading frame, separated by a short linker. These dimers were constructed from two types of  $\alpha$ -subunits and the  $\beta$ -subunit. One of the  $\alpha$ -subunits ( $\alpha_m$ ) was mutant, containing a deletion in the amino-terminal region that strongly affects its apparent affinity for agonist (15, 16) and makes it a robust reporter for inclusion in the channel tetramer. We injected a number of combinations of these tandem dimers, alone or in pairs, and observed the characteristics of the CNG channels that formed. The conclusions of this study are predicated on certain basic assumptions: (i) CNG channels are tetramers; (ii) there is a fixed or preferred assembly of subunits, and the phenotype of expressed channels arises from a single population of channels; (iii) linking subunits together as dimers has no effect on subunit behavior and does not force assembly of subunits into an arrangement different from their preferred arrangement; (iv) when both subunits of a dimer incorporate into the channel, the subunits are neighboring; and (v) although the first subunit may, under certain circumstances, incorporate into the channel without the second subunit, the second subunit never incorporates into the channel without the first subunit. In this study, we present evidence supporting many of these assumptions, suggesting that  $\alpha+\beta$  heteromultimers have two  $\alpha$ -subunits and two  $\beta$ -subunits and that they are arranged in an  $\alpha-\alpha-\beta-\beta$  configuration.

## MATERIALS AND METHODS

The cDNA for the  $\alpha$ -subunit and the  $\beta$ -subunit of the rat olfactory CNG channel were kindly provided by the laboratories

The publication costs of this article were defrayed in part by page charge payment. This article must therefore be hereby marked "advertisement" in accordance with 18 U.S.C. §1734 solely to indicate this fact.

© 1998 by The National Academy of Sciences 0027-8424/98/9514546-6\$2.00/0  
PNAS is available online at www.pnas.org.

This paper was submitted directly (Track II) to the *Proceedings* office. Abbreviation: CNG, cyclic nucleotide-gated.

‡To whom reprint requests should be addressed. e-mail: zagotta@u.washington.edu.

of R. R. Reed (The Johns Hopkins School of Medicine, Baltimore, MD) and Kai Zinn (California Institute of Technology, Pasadena, CA), respectively. These cDNAs were separately subcloned into a high-expression vector (kindly provided by E. R. Liman, Harvard University, Boston, MA) that contains the untranslated sequences of the *Xenopus*  $\beta$ -globin gene (24). In general, the oocyte expression, solutions, and electrophysiology were like those previously described (25). Briefly, *Xenopus* oocytes were injected with *in vitro*-transcribed RNA coding for channel subunits, incubated for 3–7 days, and patch-clamped in the inside-out configuration. Intracellular and extracellular solutions contained 130 mM NaCl, 0.2 mM EDTA, and 3 mM Hepes (pH 7.2). For some experiments, niflumic acid (500  $\mu$ M) was added to the pipette (extracellular) solution to reduce endogenous  $\text{Ca}^{2+}$ -activated  $\text{Cl}^-$  currents. Cyclic nucleotides were added to the internal solution at the concentrations indicated. The  $\alpha_m$  subunit has a deletion from E50 to R92. It was generated by using a method based on PCR like that previously described (26) and was verified by sequence analysis. The first subunit of a tandem dimer was wild-type and joined to the following subunit by a 21-aa linker consisting of the sequence QQQQQQQQIEGRQQQQQQQA. The  $\alpha$ -subunit as the second subunit of a dimer was the  $\alpha_{wt}$  or  $\alpha_m$  subunit with an M2V mutation to create an *NcoI* cut/splice site. The  $\beta$ -subunit as the second subunit of a dimer had an S2G mutation to create an *NcoI* cut/splice site.

For the data presented here, dimer coinjections were done at a ratio of 1:1, and monomer coinjections at a ratio of 4:1 or 2:1 ( $\alpha$ : $\beta$ ). Data from coinjection of  $\alpha\alpha$  and  $\beta\beta$  dimers at a ratio of 4:1 were very similar to those at a ratio of 1:1, and data from coinjection of  $\alpha$  and  $\beta$  monomers at a ratio of 20:1 were similar to those at 4:1 (data not shown), indicating the ample supply of  $\beta$ -subunits to form channels of the preferred arrangement for the experiments in this study. Because of the large effect of the  $\beta$ -subunit on the apparent affinity of channels for cAMP, we can estimate an upper limit for the fractional population of channels that could have been  $\alpha$ -homomultimers in experiments that produced  $\alpha+\beta$  heteromultimers. We modeled the dose–response data from the  $\alpha\alpha+\beta\beta$  coinjections as resulting from a mixed population of these two channel types, and estimate that no more than 25% of the channels could have been  $\alpha$ -homomultimers (data not shown). All currents were tested for desensitization as shown in Fig. 2D. For those without desensitization, voltage pulses were applied every 3–5 sec. For those that desensitized, cyclic nucleotide-free solution was perfused for a minimum of 20 sec between each application of ligand. Voltage pulses were applied every 1 sec, and on application of ligand, the largest current was used for the measurement. Using this protocol, we estimate that errors from desensitization were seldom greater than 15% for any given measurement.

## RESULTS

We studied cloned rat olfactory CNG channels expressed in *Xenopus* oocytes. Several days after injecting oocytes with RNA coding for either subunit monomers or tandem dimers, we recorded CNG currents from inside-out patches pulled from oocyte membranes. Cyclic nucleotides were applied to the intracellular side of the patch, and the currents in the absence of cyclic nucleotides were subtracted. Currents were usually recorded by using a successive-pulse protocol to  $-60$  and  $60$  mV from a holding potential of  $0$  mV (Fig. 1 *Inset*). Oocytes injected with RNA coding for wild-type  $\alpha$ -subunit monomers produced CNG currents with properties very similar to those previously described for olfactory  $\alpha$ -homomultimers (Table 1; refs. 6, 27). The  $\alpha_m$  subunit lacks amino acids 50–92 in the amino-terminal region, shown to contain an autoexcitatory region that potentiates CNG channel gating and the site of modulation by  $\text{Ca}^{2+}$ /calmodulin (15, 16). Dose–response data for activation of  $\alpha_m$  homomultimers by cAMP showed that the concentration of ligand that activates half the maximum current ( $K_{1/2}$ ) is shifted to higher concentrations by about 9-fold relative to  $\alpha_{wt}$  channels. Additionally, for

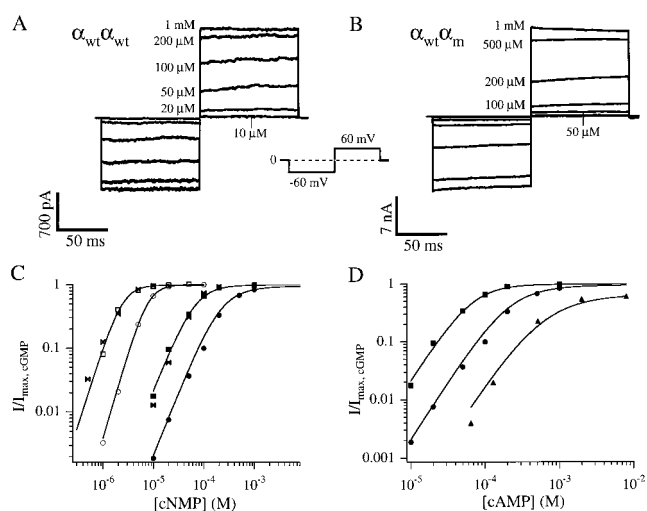
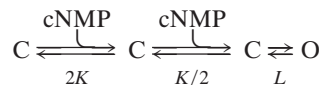


FIG. 1. Currents from injection of RNA for wild-type olfactory  $\alpha_{wt}\alpha_{wt}$  homodimers (A) and for  $\alpha_{wt}\alpha_m$  heterodimers (B) activated by a range of concentrations of cAMP. The voltage-pulse protocol is shown in the *Inset*. (C) Data are normalized dose–response relations at  $60$  mV from patches with channels from injection of  $\alpha_{wt}$  monomers (bowed),  $\alpha_{wt}\alpha_{wt}$  homodimers (squares), or  $\alpha_{wt}\alpha_m$  heterodimers (circles) for activation of the channels by cAMP (filled symbols) or cGMP (open symbols). Superimposed on the data are fits to the dimer data of Hill equations of the form  $I = I_{max} \{ [cNMP]^n / (K_{1/2}^n + [cNMP]^n) \}$ , where  $[cNMP]$  is the concentration of ligand,  $K_{1/2}$  is the concentration that produces half-maximal current, and  $n$  is the Hill slope. For  $\alpha_{wt}\alpha_{wt}$ ,  $K_{1/2} = 70 \mu\text{M}$  and  $n = 1.9$  for activation by cAMP and  $K_{1/2} = 2.4 \mu\text{M}$ , and  $n = 2.5$  for activation by cGMP and  $I_{max}$  was set to unity. For  $\alpha_{wt}\alpha_m$ ,  $K_{1/2} = 269 \mu\text{M}$ ,  $n = 2.0$  and  $I_{max} = 0.89$  for activation by cAMP, and  $K_{1/2} = 7.8 \mu\text{M}$  and  $n = 2.7$  for activation by cGMP and  $I_{max}$  was set to unity. (D) The dose–response data for activation of  $\alpha_{wt}\alpha_{wt}$  dimers (squares) and  $\alpha_{wt}\alpha_m$  dimers (circles) by cAMP are replotted from (C). Also plotted are dose–response data for activation of  $\alpha_m$  monomers (triangles) by cAMP. Superimposed on the data are fits to Scheme 1.  $K = 1050 \text{ M}^{-1}$  for all three curves. For  $\alpha_{wt}\alpha_{wt}$ ,  $L = 200$ , and for  $\alpha_m$ ,  $L = 1.86$ . The prediction of Scheme 1 for the case of a channel with two  $\alpha_{wt}$ -subunits and two  $\alpha_m$ -subunits is based on the assumption of a concerted final transition among the subunits from closed to open (19), which predicts  $L = 19.4$ . The curve superimposed on that data is this prediction.

these channels, saturating cAMP can activate only  $61 \pm 1\%$  ( $n = 6$ ) of the current activated by cGMP, compared with  $\alpha_{wt}$  channels that can produce as much current by saturating cAMP as by cGMP ( $I_{max, cAMP} / I_{max, cGMP} = 0.98 \pm 0.02$ ,  $n = 12$ ) (Fig. 1D; Table 1). These data indicate that expression of  $\alpha_m$  monomers yields homomeric channels with properties very similar to  $\alpha_{wt}$  channels in the presence of  $\text{Ca}^{2+}$ /calmodulin; that is, with reduced apparent affinities for cyclic nucleotide and a reduction in the maximum current elicited by saturating cAMP (15, 16).

We can understand these gating alterations by considering a simplified model of CNG channel gating (25):



Scheme 1

where C and O represent closed and open channels and  $K$  and  $L$  are the equilibrium constants for the initial binding of ligand and for the allosteric conformational change, respectively. This model considers that the opening of the channel involves the independent and identical binding of two cyclic nucleotides followed by a concerted allosteric opening transition. At saturating concentrations of cyclic nucleotide, at which the channels are fully ligand-bound, the open probability ( $P_o$ ) is given by  $L/(L + 1)$  where, in general,  $L$  depends on the channel and on the ligand. For homomeric  $\alpha_{wt}$  and homomeric  $\alpha_m$  channels,  $L$  is so large for

Table 1. Gating parameters of channels from injections of the indicated RNA

RNA injected	$K_{1/2}$ , $\mu\text{M}$				$n$ (60 mV)		$I_{-60\text{mV}}/I_{60\text{mV}}$		Desensitization
	cAMP		cGMP		cAMP	cGMP	cAMP	cGMP	
	60 mV	-60 mV	60 mV	-60 mV					
$\alpha_{\text{wt}}$ mono	$83 \pm 3$ $n = 26$	$89 \pm 3$ $n = 26$	$2.77 \pm 0.13$ $n = 10$	$2.85 \pm 0.11$ $n = 10$	$2.33 \pm 0.06$ $n = 25$	$2.56 \pm 0.07$ $n = 10$	$0.79 \pm 0.01$ $n = 28$	$0.81 \pm 0.02$ $n = 12$	No
$\alpha_{\text{m}}$ mono	$715 \pm 51$ $n = 5$	ND	ND	ND	$1.77 \pm 0.14$ $n = 3$	ND	ND	ND	No
$\alpha_{\text{wt}} + \beta$ mono	$10.5 \pm 0.8$ $n = 20$	$16.9 \pm 1.0$ $n = 20$	$5.2 \pm 1.2$ $n = 4$	$12.8 \pm 1.6$ $n = 4$	$1.5 \pm 0.1$ $n = 20$	$1.3 \pm 0.1$ $n = 4$	$0.51 \pm 0.01$ $n = 44$	$0.49 \pm 0.02$ $n = 29$	Yes
$\alpha_{\text{m}} + \beta$ mono	$53 \pm 3$ $n = 5$	$82 \pm 10$ $n = 5$	$12 \pm 1$ $n = 2$	$21 \pm 1$ $n = 2$	$1.46 \pm 0.05$ $n = 5$	$1.36 \pm 0.07$ $n = 5$	$0.60 \pm 0.02$ $n = 4$	$0.54 \pm 0.02$ $n = 2$	Yes
$\alpha_{\text{wt}}\alpha_{\text{wt}}$	$65 \pm 2$ $n = 7$	$76 \pm 5$ $n = 7$	$2.3 \pm 0.2$ $n = 7$	$2.4 \pm 0.2$ $n = 7$	$2.06 \pm 0.07$ $n = 7$	$2.56 \pm 0.08$ $n = 7$	$0.78 \pm 0.1$ $n = 7$	$0.81 \pm 0.01$ $n = 7$	No
$\alpha_{\text{wt}}\alpha_{\text{m}}$	$257 \pm 8$ $n = 16$	$274 \pm 8$ $n = 16$	$8.9 \pm 0.3$ $n = 15$	$9.5 \pm 0.4$ $n = 15$	$2.30 \pm 0.04$ $n = 16$	$2.79 \pm 0.04$ $n = 15$	$0.77 \pm 0.01$ $n = 15$	$0.79 \pm 0.01$ $n = 15$	No
$\alpha_{\text{wt}}\alpha_{\text{wt}} + \beta\beta$	$8.5 \pm 0.4$ $n = 14$	$18.5 \pm 1.5$ $n = 14$	$5.6 \pm 0.3$ $n = 11$	$9.9 \pm 1.2$ $n = 10$	$1.36 \pm 0.05$ $n = 14$	$1.19 \pm 0.06$ $n = 14$	$0.57 \pm 0.01$ $n = 13$	$0.52 \pm 0.02$ $n = 9$	Yes
$\alpha_{\text{wt}}\alpha_{\text{m}} + \beta\beta$	$28.4 \pm 3.7$ $n = 14$	$47.6 \pm 4.4$ $n = 14$	$9.1 \pm 1.1$ $n = 10$	$9.3 \pm 1.1$ $n = 9$	$1.21 \pm 0.07$ $n = 14$	$1.61 \pm 0.10$ $n = 10$	$0.62 \pm 0.02$ $n = 14$	$0.57 \pm 0.04$ $n = 9$	Yes
$\alpha_{\text{wt}}\alpha_{\text{wt}} + \beta\alpha_{\text{wt}}$	$15.3 \pm 1.7$ $n = 7$	$21.4 \pm 1.9$ $n = 5$	$3.5 \pm 0.5$ $n = 5$	$4.4 \pm 0.5$ $n = 4$	$1.26 \pm 0.11$ $n = 7$	$1.16 \pm 0.06$ $n = 5$	$0.55 \pm 0.02$ $n = 5$	$0.60 \pm 0.02$ $n = 4$	Yes
$\alpha_{\text{wt}}\alpha_{\text{wt}} + \beta\alpha_{\text{m}}$	$11.8 \pm 1.3$ $n = 10$	$19.6 \pm 2.2$ $n = 7$	$4.6 \pm 0.5$ $n = 4$	$8.1 \pm 1.1$ $n = 5$	$1.41 \pm 0.07$ $n = 8$	$1.50 \pm 0.08$ $n = 4$	$0.54 \pm 0.02$ $n = 7$	$0.54 \pm 0.03$ $n = 4$	Yes
$\alpha_{\text{wt}}\alpha_{\text{m}} + \beta\alpha_{\text{m}}$	$33.6 \pm 5.2$ $n = 10$	$46.9 \pm 3.6$ $n = 10$	$7.4 \pm 0.3$ $n = 9$	$8.4 \pm 0.6$ $n = 9$	$1.25 \pm 0.04$ $n = 10$	$1.18 \pm 0.04$ $n = 10$	$0.64 \pm 0.01$ $n = 10$	$0.62 \pm 0.02$ $n = 9$	Yes

The first six parameters are from fits of the data to Hill equations of the form in Fig. 1. The current ratios are ratios of the  $I_{\text{max}}$  from the Hill equations fits, and are thus saturating currents elicited by cAMP or cGMP. Desensitization was measured by observing any current decline during successive brief depolarizations to 60 mV, applied 1/sec. Injections of  $\alpha_{\text{wt}}\beta$ ,  $\beta\alpha_{\text{wt}}$ ,  $\beta\alpha_{\text{m}}$ ,  $\beta\beta$ , and coinjections of  $\alpha_{\text{wt}}\beta$  and  $\beta\alpha_{\text{wt}}$ , and  $\alpha_{\text{wt}}\beta$  and  $\beta\alpha_{\text{m}}$  dimers failed to elicit CNG currents, with a minimum of 10 oocytes tested for each. ND, not done.

cGMP-bound channels that at saturating cGMP, the fractional activation is very near unity. The potentiation by the autoexcitatory region contained within the deletion in  $\alpha_{\text{m}}$  involves an interaction of this region with the cyclic nucleotide-binding region that increases by about 100-fold the equilibrium constant,  $L$ , of the allosteric conformational change (15). Thus, this deletion, or the presence of  $\text{Ca}^{2+}$ /calmodulin, strongly decreases  $L$ , and this reduction is manifested in two ways: (i) a shift in the apparent affinity for activation of the channel by ligand to higher concentrations and (ii) for a case like cAMP, in which  $L$  is smaller, a marked reduction in the maximum current at saturating ligand. Thus, for unmodulated cAMP-bound wild-type  $\alpha$ -channels,  $L$  has a value of about 100–200 (28), and so a 100-fold reduction in  $L$ , as for  $\alpha_{\text{m}}$  channels or wild-type channels in the presence of  $\text{Ca}^{2+}$ /calmodulin, gives an  $L$  near 1, and thus a fractional activation around half-maximal.

We constructed tandem dimers from three different rat olfactory CNG channel subunits: wild-type  $\alpha$ -subunits ( $\alpha_{\text{wt}}$ ), mutant  $\alpha$ -subunits ( $\alpha_{\text{m}}$ ), and wild-type  $\beta$ -subunits. Injection of RNA for tandem  $\alpha_{\text{wt}}\alpha_{\text{wt}}$  dimers produced currents indistinguishable from those produced by  $\alpha_{\text{wt}}$  monomers in all respects, including the  $K_{1/2}$  for activation by cAMP and cGMP, the slope of the dose–response relation, and rectification (Fig. 1 A and C; Table 1). Injection of RNA for tandem  $\alpha_{\text{wt}}\alpha_{\text{m}}$  dimers produced currents similar to those from  $\alpha_{\text{wt}}\alpha_{\text{wt}}$  dimers or  $\alpha_{\text{wt}}$  monomers, but with apparent affinities for both cAMP and cGMP shifted to about 3-fold higher concentrations, and a small reduction in the maximum current elicited by saturating cAMP relative to cGMP ( $I_{\text{max, cAMP}}/I_{\text{max, cGMP}} = 0.84 \pm 0.02$ ,  $n = 15$ ) (Fig. 1 B and C; Table 1). In Fig. 1D are plotted dose–response data for  $\alpha_{\text{wt}}\alpha_{\text{wt}}$  dimers,  $\alpha_{\text{wt}}\alpha_{\text{m}}$  dimers, and  $\alpha_{\text{m}}$  monomers for activation by cAMP. Superimposed on the data are curves for fits of the data to the model of Scheme 1. The  $\alpha_{\text{m}}$  data were fit with a value of  $L$  reduced by about a factor of 100, relative to that for  $\alpha_{\text{wt}}\alpha_{\text{wt}}$ , while keeping  $K$  the same. The  $\alpha_{\text{wt}}\alpha_{\text{m}}$  data were fit with  $K$  again kept constant and  $L$  set to the geometric mean between its values for  $\alpha_{\text{wt}}\alpha_{\text{wt}}$  and  $\alpha_{\text{m}}$ , which is just what Scheme 1 predicts for a channel with a

concerted opening transition that contains two wild-type and two mutant subunits (19). Thus, the altered gating of the  $\alpha_{\text{m}}$  subunits acts as a reporter, verifying their inclusion in the tetramer, and the physical link between the  $\alpha_{\text{wt}}$  and  $\alpha_{\text{m}}$  subunits makes a  $\alpha_{\text{wt}}\alpha_{\text{m}}\alpha_{\text{wt}}\alpha_{\text{m}}$  arrangement the most likely possibility (Fig. 5).

Fig. 2A shows data from an experiment with coinjection of  $\alpha_{\text{wt}}\alpha_{\text{wt}}$  and  $\beta\beta$  dimers into the same oocyte. Heteromeric  $\alpha + \beta$  channels differ from homomeric  $\alpha$  channels in a number of signature characteristics (Table 1) (20, 22). Channels formed by  $\alpha_{\text{wt}}\alpha_{\text{wt}}$  and  $\beta\beta$  dimers were indistinguishable from channels formed by  $\alpha$  and  $\beta$  monomers in all of the characteristics that distinguish them from homomeric  $\alpha$  channels (Fig. 2A, C, and D; Table 1). These characteristics include (i) an eightfold shift in the  $K_{1/2}$  for cAMP to lower concentrations, (ii) a reduction in the slope of the dose–response curve (Hill equation slope 1.2–1.6 vs. 2.1–2.7), (iii) a more pronounced time-dependence of the current on voltage steps, (iv) desensitization when expressed in oocytes (Fig. 2D), and (v) a more pronounced rectification of the current at saturating concentrations. Collectively, these identifying characteristics clearly distinguish between channels composed of  $\alpha$ -subunits and those composed of both  $\alpha$ - and  $\beta$ -subunits and form the basis of the assigned phenotype for each combination of injected dimers (Fig. 5). Like heteromultimers formed by  $\alpha$  and  $\beta$  monomers,  $\alpha + \beta$  channels formed by dimers produce as much current with saturating cAMP as with saturating cGMP ( $I_{\text{max, cAMP}}/I_{\text{max, cGMP}} = 1.06 \pm 0.06$ ,  $n = 8$ ). Thus, coinjection of an  $\alpha\alpha$  dimer with a  $\beta\beta$  dimer yields channels indistinguishable from  $\alpha + \beta$  heteromultimers formed by monomers.

We asked whether substitution of an  $\alpha_{\text{m}}$  for an  $\alpha_{\text{wt}}$  subunit as the second subunit of an  $\alpha\alpha$  dimer shifts apparent affinities for ligand of phenotypic  $\alpha + \beta$  channels, like the results in Fig. 1 for  $\alpha$ -channels. Channels formed from coinjection of  $\alpha_{\text{wt}}\alpha_{\text{m}}$  and  $\beta\beta$  dimers resulted in currents with these same  $\alpha + \beta$  signature characteristics but with the  $K_{1/2}$  values for activation by cAMP and cGMP shifted to higher concentrations relative to channels created by coinjection of  $\alpha_{\text{wt}}\alpha_{\text{wt}}$  and  $\beta\beta$  dimers (Fig. 2 B and C; Table 1). This shift in the apparent affinities indicates that these



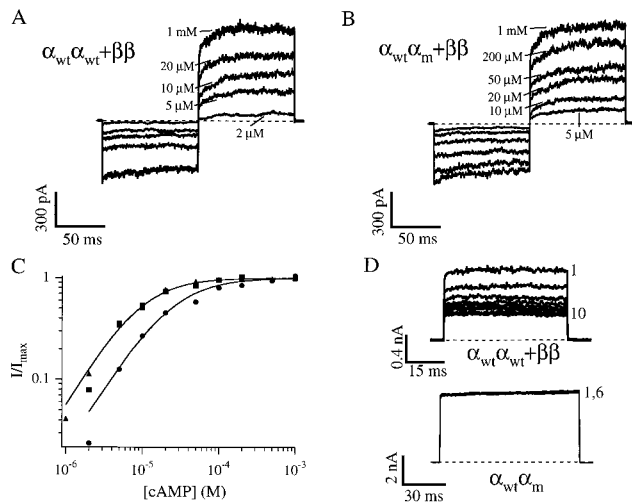


FIG. 2. Currents from coinjection of  $\alpha_{wt}\alpha_{wt}$  and  $\beta\beta$  (A) or  $\alpha_{wt}\alpha_m$  and  $\beta\beta$  (B) dimers activated by a range of concentrations of cAMP. The pulse protocol is as in Fig. 1. (C) Data are normalized dose-response relations at 60 mV from patches with channels from coinjection of  $\alpha$  and  $\beta$  monomers (triangles),  $\alpha_{wt}\alpha_{wt}$  and  $\beta\beta$  dimers (squares), or  $\alpha_{wt}\alpha_m$  and  $\beta\beta$  dimers (circles) for activation of the channels by cAMP. Superimposed on the data are fits of the dimer data to Hill equations of the form in Fig. 1. The fitted values of  $K_{1/2}$  are  $9.2 \mu\text{M}$  and  $25 \mu\text{M}$ , and of  $n$  are 1.3 and 1.4 for channels from  $\alpha_{wt}\alpha_{wt}$  and  $\beta\beta$  and  $\alpha_{wt}\alpha_m$  and  $\beta\beta$  coinjections, respectively, and  $I_{max}$  was set at unity. (D) Desensitization is shown for currents with successive brief depolarizations to 60 mV given every 1 s, in the presence of saturating cAMP, for channels from  $\alpha_{wt}\alpha_{wt}$  and  $\beta\beta$  or  $\alpha_{wt}\alpha_m$  injections. The former desensitize, like channels from  $\alpha + \beta$  monomers, but the latter do not, like channels from  $\alpha$  monomers.

channels have incorporated the  $\alpha_m$ -subunit half of the injected  $\alpha_{wt}\alpha_m$  dimer. As with channels from  $\alpha_{wt}\alpha_m$  dimers alone, the shift in the  $K_{1/2}$  value for  $\alpha + \beta$  channels suggests that both  $\alpha$ -subunits of the dimer are being incorporated and that they are adjacent. Thus, a tetrameric arrangement of  $\alpha$  and  $\beta$  subunits with two adjacent  $\alpha$ -subunits yields channels very similar to channels formed from  $\alpha$  and  $\beta$  monomers, suggesting that  $\alpha + \beta$  heteromultimers have adjacent  $\alpha$ -subunits.

Singly injecting all dimers consisting of one  $\alpha$ -subunit and one  $\beta$ -subunit failed to yield CNG currents (Table 1). These dimers would be predicted to form channels with an alternating  $\alpha\beta$  arrangement ( $\alpha - \beta - \alpha - \beta$ ). Nonexpression by itself is not strong evidence, but this result is consistent with functional  $\alpha + \beta$  channels not consisting of alternating  $\alpha$  and  $\beta$  subunits. Coinjections of  $\alpha\beta$  dimers and  $\beta\alpha$  dimers also failed to yield CNG currents.

Having demonstrated that  $\alpha + \beta$  channels have adjacent  $\alpha$ -subunits, we turned our attention to discriminating between the two remaining alternatives for subunit arrangement in a tetrameric heteromultimer containing adjacent  $\alpha$ -subunits: a channel with three  $\alpha$ -subunits and one  $\beta$ -subunit ( $\alpha - \alpha - \alpha - \beta$ ) or a channel with two adjacent  $\alpha$ -subunits and two adjacent  $\beta$ -subunits ( $\alpha - \alpha - \beta - \beta$ ). To distinguish between these two possibilities, we coinjected a dimer with two  $\alpha$ -subunits ( $\alpha\alpha$ ) with a dimer with a  $\beta$ -subunit followed by an  $\alpha$ -subunit ( $\beta\alpha$ ) (Table 1). Channels formed from these injections were  $\alpha + \beta$ -like and had behavior indistinguishable from that of channels created by coinjections of  $\alpha\alpha$  and  $\beta\beta$  dimers (Table 1; Fig. 3). Furthermore, similar to the results obtained with  $\alpha\alpha$  (Fig. 1) or  $\alpha\alpha$  and  $\beta\beta$  (Fig. 2) injections, channels formed always displayed the effect of the presence of the  $\alpha_m$ -subunit when it was the second subunit of the  $\alpha\alpha$  dimer. This effect was easily observable by the presence of the telltale shift in the apparent affinity. We also tested coinjections of  $\alpha\alpha$  and  $\alpha\beta$  dimers. Channels formed from these experiments acted much like those from injection of  $\alpha\alpha$  dimers or  $\alpha$  monomers; that is, of the  $\alpha$ -channel phenotype (data not shown). However, because we

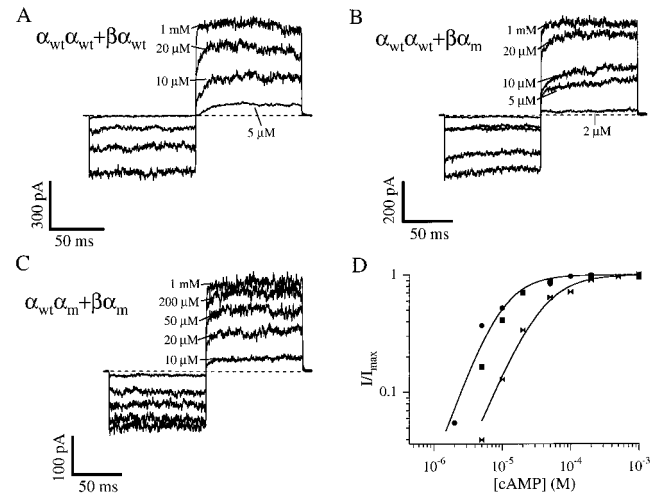


FIG. 3. Currents from coinjection of  $\alpha_{wt}\alpha_{wt}$  and  $\beta\alpha_{wt}$  (A),  $\alpha_{wt}\alpha_{wt}$  and  $\beta\alpha_m$  (B), or  $\alpha_{wt}\alpha_m$  and  $\beta\alpha_{wt}$  (C) dimers activated by a range of concentrations of cAMP. The pulse protocol is as in Figs. 1 and 2. (D) Data are normalized dose-response relations at 60 mV for patches with channels from coinjections of  $\alpha_{wt}\alpha_{wt}$  and  $\beta\alpha_m$  (circles),  $\alpha_{wt}\alpha_{wt}$  and  $\beta\alpha_{wt}$  (squares), and  $\alpha_{wt}\alpha_m$  and  $\beta\alpha_m$  (bows). Superimposed are fits of the  $\alpha_{wt}\alpha_{wt}$  and  $\beta\alpha_m$  and  $\alpha_{wt}\alpha_m$  and  $\beta\alpha_{wt}$  data to Hill equations of the form as in Fig. 1. The fitted values of  $K_{1/2}$  are  $9.8 \mu\text{M}$  and  $29 \mu\text{M}$ , and of  $n$  are 1.4 and 1.1 for channels from  $\alpha_{wt}\alpha_{wt}$  and  $\beta\alpha_m$  and  $\alpha_{wt}\alpha_m$  and  $\beta\alpha_{wt}$  injections, respectively, and  $I_{max}$  was set at unity.

cannot detect the presence of the  $\alpha\beta$  dimers either alone or in coinjections, we lack any independent evidence that these dimers are functional and are being expressed. We therefore must attach less weight to this result. The uncertain expression of  $\alpha\beta$  dimers also reduces the weight we attach to the result that coinjection of  $\alpha\beta$  and  $\beta\alpha$  dimers did not yield functional channels.

Other investigators using tandem dimers have shown that they may sometimes incorporate only the leading subunit into the channel tetramer, leaving the second subunit outside of the channel (29). We asked whether the same thing could happen here. To test for this behavior, we focused on the  $\alpha\alpha$  and  $\beta\alpha$  coinjections that produced channels closely matching the  $\alpha + \beta$  phenotype whose stoichiometry and arrangement we wished to determine. In this scenario, coinjection of  $\alpha\alpha$  and  $\beta\alpha$  dimers could result in a channel with two  $\alpha$  and two  $\beta$  subunits, with the  $\alpha$  subunits of the  $\beta\alpha$  dimers unincorporated (Fig. 5).

Using the reporting ability of the  $\alpha_m$  subunit, we examined channels formed by coinjection of  $\alpha_{wt}\alpha_{wt}$  and  $\beta\alpha_m$  dimers. If the resulting channels were of the  $\alpha - \alpha - \alpha - \beta$  arrangement, and thus were incorporating the  $\alpha_m$  subunit, we would expect to detect it by its effect on the apparent affinity. Fig. 3 shows data from coinjections of  $\alpha_{wt}\alpha_{wt}$  and  $\beta\alpha_{wt}$  (A),  $\alpha_{wt}\alpha_{wt}$  and  $\beta\alpha_m$  (B), or  $\alpha_{wt}\alpha_m$  and  $\beta\alpha_m$  (C) dimers. All three coinjection experiments produced currents with all of the signature features of  $\alpha + \beta$  channels, including increased cAMP affinity, decreased dose-response relation slope, increased time-dependence and rectification, and desensitization (Table 1). Plotted in Fig. 3D are dose-response curves for activation of the resulting channels by cAMP. There was no significant difference between the data for the channels from  $\alpha_{wt}\alpha_{wt}$  and  $\beta\alpha_m$  coinjections and those from  $\alpha_{wt}\alpha_{wt}$  and  $\beta\alpha_{wt}$  coinjections, strongly suggesting that the  $\alpha$ -subunits of the  $\beta\alpha$  dimers were not being incorporated. Data from the  $\alpha_{wt}\alpha_m$  and  $\beta\alpha_m$  coinjections show that when the  $\alpha_m$  is the second subunit of the  $\alpha\alpha$  dimer, the dose-response curve is clearly shifted to higher concentrations. They were indistinguishable from those from  $\alpha_{wt}\alpha_m$  and  $\beta\beta$  coinjections (Table 1); that is, as with channels from  $\alpha_{wt}\alpha_{wt}$  and  $\beta\beta$  dimer or  $\alpha$  and  $\beta$  monomer coinjections but with an apparent affinity shifted to about 3-fold higher concentrations. We were thus able to discriminate between the two alternatives by looking for the telltale shift in the apparent affinity

caused by the  $\alpha_m$  subunit. The results from this experiment further suggest that  $\alpha+\beta$  heteromultimers have two  $\alpha$ -subunits and two  $\beta$ -subunits in an  $\alpha-\alpha-\beta-\beta$  arrangement.

However, the data in Fig. 3 are not inconsistent with an  $\alpha-\alpha-\alpha-\beta$  arrangement if a third  $\alpha$ -subunit were to come from an  $\alpha\alpha$  dimer instead of the  $\beta\alpha$  dimer. To further examine this possibility, we recorded currents resulting from coinjections of  $\alpha_m$  and  $\beta$  monomers, and compared dose-response data from these channels with those from coinjection of  $\alpha_{wt}$  and  $\beta$  monomers or  $\alpha_{wt}\alpha_m$  and  $\beta\beta$  dimers (Fig. 4). The implications of this experiment for the  $\alpha-\alpha-\beta-\beta$  and  $\alpha-\alpha-\alpha-\beta$  scenarios are depicted in Fig. 4A. Shown schematically are the two possibilities for the case of coinjection of  $\alpha_{wt}\alpha_m$  and  $\beta\beta$  dimers. If an  $\alpha+\beta$  channel indeed has two  $\alpha$ -subunits and two  $\beta$ -subunits, then coinjection of  $\alpha_{wt}$  and  $\beta$  monomers would yield a channel with two  $\alpha_{wt}$ -subunits; coinjection of  $\alpha_m$  and  $\beta$  monomers, a channel with two  $\alpha_m$ -subunits; and coinjection of  $\alpha_{wt}\alpha_m$  and  $\beta\beta$  dimers, a channel with one  $\alpha_{wt}$ -subunit and one  $\alpha_m$ -subunit. Thus, like the comparison of  $\alpha$  channels with zero, two, or four  $\alpha_m$ -subunits (Fig. 1D), an  $\alpha-\alpha-\beta-\beta$  arrangement predicts that the apparent affinity for a channel with one  $\alpha_{wt}$ -subunit and one  $\alpha_m$ -subunit would be the geometric mean between that for a channel with zero and two  $\alpha_m$ -subunits (Fig. 4B). On the other hand, for coinjection of  $\alpha\alpha$  and  $\beta\beta$  dimers to yield an  $\alpha+\beta$  channel with three  $\alpha$ -subunits and one  $\beta$ -subunit (Fig. 4A, Right), the first  $\alpha$ -subunit only of an  $\alpha\alpha$  dimer, but not the second, and the first  $\beta$ -subunit only of a  $\beta\beta$

dimer, but not the second, would have to incorporate. Thus, this scenario predicts that coinjection of  $\alpha_{wt}$  and  $\beta$  monomers would yield a channel with three  $\alpha_{wt}$ -subunits; coinjection of  $\alpha_m$  and  $\beta$  monomers, a channel with three  $\alpha_m$ -subunits; and coinjection of  $\alpha_{wt}\alpha_m$  and  $\beta\beta$  dimers, a channel with two  $\alpha_{wt}$ -subunits and one  $\alpha_m$ -subunit. This scenario would thus require that the ratio of the  $K_{1/2}$  values of channels from coinjections of  $\alpha_{wt}$  and  $\beta$  monomers and  $\alpha_m$  and  $\beta$  monomers not be the square of the ratio of its values from coinjections of  $\alpha_{wt}$  and  $\beta$  monomers and  $\alpha_{wt}\alpha_m$  and  $\beta\beta$  dimers, but the cube of that ratio (Fig. 4B). However, the data from coinjection of  $\alpha_m$  and  $\beta$  monomers indicate a change in the apparent affinity very nearly the square of the ratio of its values from coinjections of  $\alpha_{wt}$  and  $\beta$  monomers and  $\alpha_{wt}\alpha_m$  and  $\beta\beta$  dimers. Thus, the model prediction from the  $\alpha-\alpha-\beta-\beta$  arrangement fits the data well. This experiment further argues against a  $\alpha-\alpha-\alpha-\beta$  configuration and further supports the  $\alpha-\alpha-\beta-\beta$  arrangement.

## DISCUSSION

Tandem subunits have also been used to show the tetrameric nature of voltage-gated  $K^+$  channels (24), inward rectifier  $K^+$  channels (30), and CNG channels (17–19). In all of these cases, and in the present work, a mutant subunit was used whose presence in the channel produces obvious effects and so acted as a reporter for its incorporation into the tetramer. We define two channel phenotypes,  $\alpha$  channels and  $\alpha+\beta$  channels, based on a set of defining characteristics that differentiate the two. We exploited the characteristic fingerprint of  $\alpha+\beta$  channels to distinguish which dimer injections produce  $\alpha+\beta$  heteromeric channels and which produce  $\alpha$  homomeric channels. In addition, the shift of the apparent affinity of the mutant  $\alpha$ -subunit made it a reporter for incorporation of the second subunit of a dimer in the channel tetramer, the major uncertainty of the tandem dimer approach. An advantage of this study is that it determined the arrangement of functional CNG channels; that is, those that produced current on application of cyclic nucleotides. Broillet and Firestein (31) showed that the olfactory  $\beta$ -subunit can form homomeric channels gated not by cyclic nucleotides but by nitric oxide. Thus, even if multimers with arrangements other than those suggested here form in the oocyte membrane, we did not observe evidence that they are cyclic nucleotide-activatable channels.

Fig. 5 shows a summary of the results of the experiments presented in this work. For each injection or coinjection, we assign a phenotype of  $\alpha$  channels or  $\alpha+\beta$  channels based on their collection of signature differences. Shown in the center column is the arrangement of the subunits for the channels formed, as deduced from the data. For all injections involving  $\alpha\alpha$  dimers, both subunits of the  $\alpha\alpha$  dimers incorporated in the channel tetramer. For those involving coinjections of  $\alpha\alpha$  dimers and  $\beta\alpha$  dimers, we deduce that only the initial  $\beta$ -subunit of the  $\beta\alpha$  dimer is being incorporated, forming an  $\alpha+\beta$  channel with two  $\alpha$  subunits and two  $\beta$  subunits. If the  $\alpha\beta$  dimers are indeed functional and being expressed, then only the initial  $\alpha$ -subunit of the  $\alpha\beta$  dimer is being incorporated, forming a tetramer with four  $\alpha$ -subunits. Thus, taken together, all of the evidence indicates that  $\alpha+\beta$  channels are composed of subunits in an  $\alpha-\alpha-\beta-\beta$  arrangement.

These experiments also provide evidence supporting the assumptions of a fixed or preferred assembly of  $\alpha+\beta$  subunits and that the phenotype of expressed channels arises from a single population. This evidence includes (i) the lack of variability in the  $K_{1/2}$  for cAMP for channels of the  $\alpha+\beta$  phenotype, even for different  $\alpha:\beta$  injection ratios of monomer and dimer RNA (data not shown), (ii) the close similarity of the data for channels from  $\alpha_{wt}\alpha_{wt}$  and  $\beta\beta$  dimers and  $\alpha$  and  $\beta$  monomers (Fig. 2; Table 1), and (iii) the lack of any effect caused by the  $\alpha$ -subunit of the  $\beta\alpha$  dimer being wild-type or mutant (Fig. 3). Our results also show that dimerization of subunits has no significant effect on  $\alpha$ - and  $\beta$ -subunit types and does not force assembly of subunits into an arrangement different from their preferred arrangement. We feel

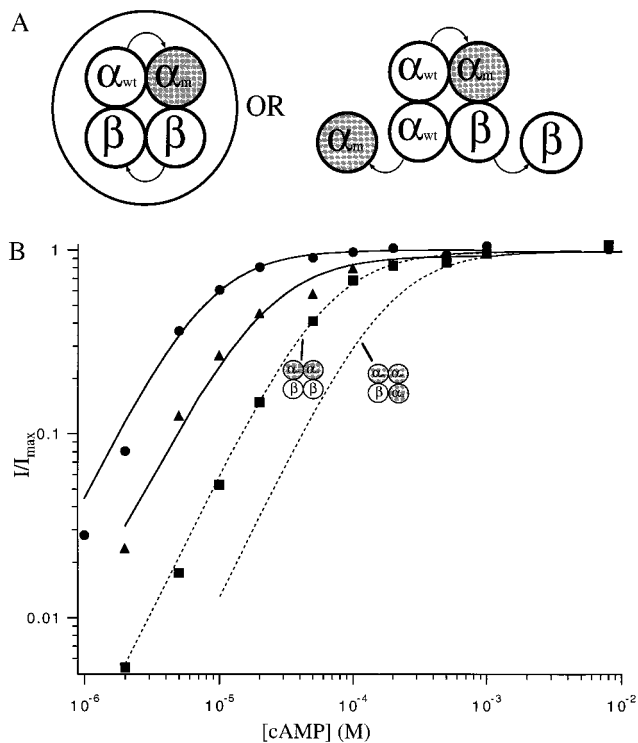


FIG. 4. (A) Schematic diagram of how  $\alpha_{wt}\alpha_m$  and  $\beta\beta$  dimer coinjections could produce channels with an arrangement of two  $\alpha$ -subunits and two  $\beta$ -subunits (Left) or three  $\alpha$ -subunits and one  $\beta$ -subunit (Right). (B) Dose-response data for activation by cAMP of channels from coinjection of  $\alpha_{wt}$  and  $\beta$  monomers (circles),  $\alpha_{wt}\alpha_m$  and  $\beta\beta$  dimers (triangles), and  $\alpha_m$  and  $\beta$  monomers (squares). The solid lines are the Hill fits to the  $\alpha_{wt}$  and  $\beta$  monomer data and the  $\alpha_{wt}\alpha_m$  and  $\beta\beta$  dimer data. For  $\alpha_{wt}$  and  $\beta$  monomers,  $K_{1/2} = 7.7 \mu\text{M}$  and  $n = 1.5$ . For  $\alpha_{wt}\alpha_m$  and  $\beta\beta$  dimers,  $K_{1/2} = 22 \mu\text{M}$  and  $n = 1.4$ . For  $\alpha_m$  and  $\beta$  monomers (Hill fit not shown for clarity),  $K_{1/2} = 63 \mu\text{M}$  and  $n = 1.5$ . The dashed line on the left is the prediction (see Methods) for the  $\alpha-\alpha-\beta-\beta$  arrangement shown on the Left in A and is a Hill equation curve with  $K_{1/2} = 63 \mu\text{M}$  and  $n = 1.5$ . The dotted line on the right is the prediction for the  $\alpha-\alpha-\alpha-\beta$  arrangement shown on the Right in (A), and is a Hill equation curve with  $K_{1/2} = 178 \mu\text{M}$  and  $n = 1.5$ . The encircled arrangement is the one best supported by the data.







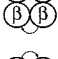
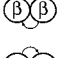

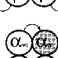
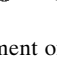
RNA injected	Deduced arrangement	Phenotype
$\alpha_{wt}$ monomer		$\alpha$ channels Wild-type affinity
$\alpha_m$ monomer		$\alpha$ channels Mutant affinity
$\alpha_{wt} + \beta$ monomers		$\alpha + \beta$ channels Wild-type affinity
$\alpha_m + \beta$ monomers		$\alpha + \beta$ channels Mutant affinity
$\alpha_{wt}\alpha_{wt}$		$\alpha$ channels Wild-type affinity
$\alpha_{wt}\alpha_m$		$\alpha$ channels Partial mutant affinity
$\alpha_{wt}\alpha_{wt} + \beta\beta$		$\alpha + \beta$ channels Wild-type affinity
$\alpha_{wt}\alpha_m + \beta\beta$		$\alpha + \beta$ channels Partial mutant affinity
$\alpha_{wt}\alpha_{wt} + \beta\alpha_{wt}$		$\alpha + \beta$ channels Wild-type affinity
$\alpha_{wt}\alpha_{wt} + \beta\alpha_m$		$\alpha + \beta$ channels Wild-type affinity
$\alpha_{wt}\alpha_m + \beta\alpha_m$		$\alpha + \beta$ channels Partial mutant affinity

FIG. 5. Deduced arrangement of the channels formed from all of the injections and coinjections. The assignment of phenotype was based on the evidence discussed in the text. "Wild-type affinity," "mutant affinity," and "partial mutant affinity" refer to channels that show behavior consistent with none, all, or half of their  $\alpha$ -subunits being  $\alpha_m$ -subunits. The  $\alpha_m$ -subunits are shaded.

that the close similarity of dose-response data between  $\alpha_{wt}\alpha_{wt}$  dimers and  $\alpha_{wt}$  monomers (Fig. 1) and between  $\alpha_{wt}\alpha_{wt}$  and  $\beta\beta$  dimers and  $\alpha$  and  $\beta$  monomers (Fig. 2) makes an effect of dimerization, *per se*, unlikely. We also never saw evidence that the second subunit of a dimer can incorporate into the channel without the first subunit. This conclusion has been reached by others. Liu *et al.* (17), using tandem dimers of rod and fish olfactory CNG  $\alpha$ -subunits, tested for preferential incorporation into channel tetramers. McCormack *et al.* (29), using Shaker-type  $K^+$  channels, found preferential incorporation of the leading subunit. Thus, no study using tandem dimers (including this work) reports preferential incorporation of the second subunit of a dimer in the channel.

Recently, it has been suggested that CNG channels gate not as a concerted opening transition involving all of the subunits, but rather that the four subunits in the tetramer may associate and activate as two independent dimers (32). For the case of  $\alpha$  channels the difference in channel behavior predicted by a strictly concerted gating scheme and the coupled dimer scheme of Liu *et al.* (32) may be relatively subtle. However, for the general case of  $\alpha + \beta$  heteromultimers, channel gating as two independent dimers may explain our finding that heteromultimers are composed of adjacent pairs of like subunits. That is, if  $\alpha + \beta$  channels do indeed open via this mechanism, it may be that only adjacent, like subunits can undergo the opening conformational change as a coupled dimer, but not  $\alpha\beta$  or  $\beta\alpha$  dimers. Thus, a tetramer with an alternating  $\alpha - \beta - \alpha - \beta$  arrangement would not yield functional CNG channels.

The question of what mechanism constrains subunit assembly in CNG channels is an interesting, and open, one. In voltage-gated  $K^+$  channels, hydrophilic amino-terminal domains guide assembly of subunits within subfamilies, and restrict cross-subfamily assembly (33). However, biochemical experiments on CNG channels similar to those in  $K^+$  channels fail to show amino-terminal-amino-terminal interactions of this kind (15, 34). Recently, it has been shown that the native olfactory channel may contain an alternatively spiced variant of the rod  $\beta$ -subunit, in addition to the olfactory  $\beta$ -subunit (35), and that olfactory heteromultimers containing the rod  $\beta$ -subunit behave remarkably similar to channels containing only olfactory  $\alpha$  and  $\beta$ -subunits (35, 36). Indeed, the apparent lack of a subunit assembly-guiding domain on CNG channels may explain why many different types of CNG channel subunits can coassemble to form functional channels (36). Our experiments indicate that heteromeric  $\alpha + \beta$  channels preferentially assemble in an  $\alpha - \alpha - \beta - \beta$  arrangement. The structural mechanism determining this preferential arrangement remains unknown.

We thank G. Eaholtz, A. Fodor, K. Matulef, L. Sunderman, and M. Varnum for comments on the manuscript, K. Black and H. Utsugi for technical assistance, and LeGay Sheridan for clerical assistance. This work was supported by the Human Frontiers Science Program and by Grant 5R01-EY10329-04 from the National Institutes of Health. W.N.Z. is an assistant investigator for the Howard Hughes Medical Institute.

- Fesenko, E. E., Kolesnikov, S. S. & Lyubarsky, A. L. (1985) *Nature (London)* **313**, 310–313.
- Nakamura, T. & Gold, G. H. (1987) *Nature (London)* **325**, 442–444.
- Yau, K. W. & Baylor, D. A. (1989) *Annu. Rev. Neurosci.* **12**, 289–327.
- Zufall, F., Firestein, S. & Shepherd, G. M. (1994) *Annu. Rev. Biophys. Biomol. Struct.* **23**, 577–607.
- Kaupp, U. B., Niidome, T., Tanabe, T., Terada, S., Bonigk, W., Stuhmer, W., Cook, N. J., Kangawa, K., Matsuo, H., Hirose, *et al.* (1989) *Nature (London)* **342**, 762–766.
- Dhallan, R. S., Yau, K. W., Schrader, K. A. & Reed, R. R. (1990) *Nature (London)* **347**, 184–187.
- Ludwig, J., Margalit, T., Eismann, E., Lancet, D. & Kaupp, U. B. (1990) *FEBS Lett.* **270**, 24–29.
- McCoy, D. E., Guggino, S. E. & Stanton, B. A. (1995) *Kidney Int.* **48**, 1125–1133.
- Biel, M., Zong, X., Distler, M., Bosse, E., Klugbauer, N., Murakami, M., Flockerzi, V. & Hofmann, F. (1994) *Proc. Natl. Acad. Sci. USA* **91**, 3505–3509.
- Weyand, I., Godde, M., Frings, S., Weiner, J., Muller, F., Altenhofen, W., Hait, H. & Kaupp, U. B. (1994) *Nature (London)* **368**, 859–863.
- Zufall, F., Shepherd, G. M. & Barnstable, C. J. (1997) *Curr. Opin. Neurobiol.* **7**, 404–412.
- Rieke, F. & Schwartz, E. A. (1994) *Neuron* **13**, 863–873.
- Anholt, R. R. (1993) *Crit. Rev. Neurobiol.* **7**, 1–22.
- Parent, A., Schrader, K., Munger, S. D., Reed, R. R., Linden, D. J. & Ronnett, G. V. (1998) *J. Neurophysiol.* **79**, 3295–3300.
- Varnum, M. D. & Zagotta, W. N. (1997) *Science* **278**, 110–113.
- Liu, M., Chen, T. Y., Ahamed, B., Li, J. & Yau, K. W. (1994) *Science* **266**, 1348–1354.
- Liu, D. T., Tibbs, G. R. & Siegelbaum, S. A. (1996) *Neuron* **16**, 983–990.
- Gordon, S. E. & Zagotta, W. N. (1995) *Proc. Natl. Acad. Sci. USA* **92**, 10222–10226.
- Varnum, M. D. & Zagotta, W. N. (1996) *Biophys. J.* **70**, 2667–2679.
- Bradley, J., Li, J., Davidson, N., Lester, H. A. & Zinn, K. (1994) *Proc. Natl. Acad. Sci. USA* **91**, 8890–8894.
- Chen, T. Y., Peng, Y. W., Dhallan, R. S., Ahamed, B., Reed, R. R. & Yau, K. W. (1993) *Nature (London)* **362**, 764–767.
- Liman, E. R. & Buck, L. B. (1994) *Neuron* **13**, 611–621.
- Berghard, A., Buck, L. B. & Liman, E. R. (1997) *Neuron* **18**, 951–958.
- Liman, E. R., Tytgat, J. & Hess, P. (1992) *Neuron* **9**, 861–871.
- Gordon, S. E. & Zagotta, W. N. (1995) *Neuron* **14**, 857–864.
- Gordon, S. E. & Zagotta, W. N. (1995) *Neuron* **14**, 177–183.
- Zagotta, W. N. & Siegelbaum, S. A. (1996) *Annu. Rev. Neurosci.* **19**, 235–263.
- Fodor, A. A., Black, K. D. & Zagotta, W. N. (1997) *J. Gen. Physiol.* **110**, 591–600.
- McCormack, K., Lin, L., Iverson, L., Tanouye, M. & Sigworth, F. (1992) *Biophys. J.* **63**, 1406–1411.
- Yang, J., Jan, Y. N. & Jan, L. Y. (1995) *Neuron* **15**, 1441–1447.
- Broillet, M. C. & Firestein, S. (1997) *Neuron* **18**, 951–958.
- Liu, D. T., Tibbs, G. R., Paoletti, P. & Siegelbaum, S. A. (1998) *Neuron* **21**, 235–248.
- Li, M., Jan, Y. N. & Jan, L. Y. (1992) *Science* **257**, 1225–1230.
- Gordon, S. E., Varnum, M. D. & Zagotta, W. N. (1997) *Neuron* **19**, 431–441.
- Sautter, A., Zong, X., Hofmann, F. & Biel, M. (1998) *Proc. Natl. Acad. Sci. USA* **95**, 4696–4701.
- Finn, J. T., Krautwurst, D., Schroeder, J. E., Chen, T.-Y., Reed, R. R. & Yau, K.-W. (1998) *Biophys. J.* **74**, 1333–1345.